

A hypothesis for the basis of the pro-oxidant nature of calcium ions

Ryan Hutcheson, Mark D. Engelmann & I. Francis Cheng*

Department of chemistry, University of Idaho, Moscow, ID 83844-2343.

**Author for correspondence (Tel.: 208-885-6387, Fax: 208-885-6173, E-mail: ifcheng@uidaho.edu)*

Received 3 November 2003; accepted 24 February 2004; Published online October

Key words: Calcium, hypothesis, reactive oxygen species, Fenton reaction, iron, EDTA, citrate, NTA, voltammetry, pH-distribution diagram

Abstract

A new hypothesis describing the role of the redox inactive Ca^{2+} ion in the expression of physiological oxidative damage is described. The hypothesis is based on the optimization of the chelation characteristics of iron complexes for pro-oxidant activity. In a previous investigation it was found that an excess of ligand kinetically hindered the Fenton reaction activity of the $\text{Fe}^{\text{II/III}}$ EDTA complex (Bobier *et al.* 2003). EDTA, citrate, NTA, and glutamate were selected as models for the coordination sites likely encountered by mobile iron, i.e. proteins. The optimal $[\text{EDTA}]:[\text{Fe}^{\text{III}}]$ ratio for Fenton reaction activity as measured by electrocatalytic voltammetry in a solution was found to be 1:1. An excess of EDTA in the amount of 10:1 [ligand]:[metal] suppresses the Fenton reaction activity to nearly the control. It is expected that the physiological coordination characteristics of mobile Fe would have a very large excess of [ligand]:[metal] and thus not be optimized for the Fenton reaction. Introduction of Ca^{2+} in to a ratio of 10:10:1 $[\text{Ca}^{2+}]:[\text{EDTA}]:[\text{Fe}^{\text{III}}]$ to the system reinvigorated the Fenton reaction activity to nearly the value of the optimal 1:1 $[\text{EDTA}]:[\text{Fe}^{\text{III}}]$ complex. The pH distribution diagrams of Ca^{2+} in the presence of EDTA and $\text{Fe}^{\text{II/III}}$ indicate that Ca^{2+} has the ability to uptake excess EDTA without displacing either Fe^{II} of Fe^{III} from their respective complexed forms. The similarity in the presence for hard ligand sites albeit with a lower binding constant for Ca^{2+} accounts for this action.

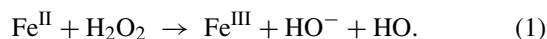
Introduction

The biochemical role of calcium is diverse. Besides its well-known functions in bone tissue and exoskeletons, calcium ions have roles in the signaling and the induction of biochemical processes. Membrane bound Ca^{2+} channels, which regulate the flow of these ions in and out of cells, are important targets in the design of new drugs. Among the important roles associated with Ca^{2+} are its roles in apoptosis, and inflammation (Krebs 1998). Disruption of Ca^{2+} homeostasis in mitochondria is hypothesized as a key step in apoptosis. The inflammatory response mechanism releases Ca^{2+} , along with reactive oxygen species (ROS) (e.g. H_2O_2 , O_2^-), histamines, and glutamate (Babior 2000). In both inflammation and in apoptosis, pro-oxidant actions are associated with increases in cellular Ca^{2+} concentration (Lee & Kang 2002). This is observed

both in plant and animal cells. Whether its presence is due to a cause or effect relationship with ROS release remains unclear, but recent experiments aimed at precisely timing the events of the inflammatory response place the initial Ca^{2+} flux preceding ROS appearance (Atlante *et al.* 2001, Caro & Cederbaum 2002a, Caro & Cederbaum 2002b). Thus, it reasons that the calcium flux is likely the cause of ROS generation, rather than an effect of ROS damage. A fundamental question arises, how does a seemingly redox inactive ion, Ca^{2+} exert a pro-oxidative influence? Calcium ions have been hypothesized as a signaling agent in the events that lead up to the oxidative events. In this contribution we propose that Ca^{2+} exerts a pro-oxidative influence in conjunction with the chelation characteristics of Fe^{II} (Bobier *et al.* 2003).

Iron complexes and iron containing enzymes figure prominently in biological oxidations. The enzymes

associated with inflammatory responses, nitric oxide synthase, myeloperoxidase, and NADPH oxidase are all important to the production of ROS and are based on iron-heme complexes (Babior 2000). Iron also has a Janus-like paradox in that while being a biologically essential element, it is also involved in collateral damage to physiological components. The Fenton Reaction (below) figures prominently into this damage.



The hydroxyl radical is the ultimate oxidant derived in the activation of O_2 . Along with a suitable iron center the hydroxyl radical has the ability to react with almost any organic with diffusion-limited kinetics and is thought to be a significant agent in the pathogenesis of many diseases (Blokina *et al.* 2003, Crichton & Pierre 2001, Welch *et al.* 2002, Arouma & Halliwell 1988, Shi *et al.* 1991, Smith *et al.* 1997, Zhao *et al.* 1994). Of particular concern is the release of iron into the low molecular weight (LMW-Fe) pool from enzymes and other physiological components (Petrat *et al.* 2002, Lehnen *et al.* 2002, Kakhlon & Cabantchick 2002, Wiseman & Halliwell 1996). Release of iron is made possible by the oxidation of the native ligand, either by enzymatic process, or by HO^\cdot (Wang & Ortiz 2003, Avila *et al.* 2000, Collins 2002, Comporti *et al.* 2002, Richards & Dettman 2003). The released iron is quickly chelated by a broad array of low molecular weight sequestering agents present in extra- and intra-cellular fluids, e.g., simple nucleotides, citrates, amino acids, and proteins (Lipscom *et al.* 1998, Sergeant *et al.* 1997, Fahn & Cohen 1992, Zhan *et al.* 1990, Weaver & Pollack, 1989, 1990). Almost without exception these LMW-Fe species are capable of the Fenton reaction and thus add to the damage of physiological components.

In a previous study, it was demonstrated that the Fenton reaction activity of the iron complexes of ethylenediaminetetraacetic acid (EDTA), diethylenetriaminepentaacetic acid (DTPA), and citrate was highly dependent on the ligand to metal concentration ratios ($[\text{L}]:[\text{M}]$) (Bobier *et al.* 2003). At molar ratios where the ligand and metal ratios are nearly equal, ability to drive the Fenton reaction was optimal. At high ligand to metal molar ratios the ability to drive the Fenton reaction was nearly absent. Formal reduction potentials of the complexes in conjunction with stability constant speciation calculations both predict that the three aforementioned complexes of iron should indeed generate hydroxyl radicals via the Fenton reaction. It was

concluded that a molar excess of ligand relative to iron represents a kinetic barrier to H_2O_2 reduction. Accepted pH species distribution diagrams for Fe^{II} and Fe^{III} EDTA complexes demonstrate only 1:1 metal:ligand structures. However, we hypothesize that higher concentrations of ligand ties up the chelation sphere of the metal center (Bobier *et al.* 2003). This prevents a direct coordination of HOOH to the metal ($\beta = 10^4$ $\text{Fe}^{\text{III}}\text{-OO[EDTA]}^{2-}$), which may be important since, it has been previously suggested that direct coordination of HOOH to a metal center is a requirement for the reduction of the O-O bond (Berlett *et al.* 1990, Bobier *et al.* 2003, Walling *et al.* 1970). Given the moderate binding constant of 10^4 , it is possible that excess EDTA may displace $-\text{O}-\text{O}^{2-}$ from the Fe^{III} center.

The occurrence of a localized increase in calcium concentration in the presence of iron will effect the L:M ratio of any iron complexes within the vicinity. It can be shown that calcium, when present in vast excess with iron and several equivalents of EDTA (relative to the iron), will be bound by the excess EDTA leaving an Fe:EDTA ratio of unity. The binding constant (β) for Fe^{II} , Fe^{III} , and Ca^{2+} with EDTA are $10^{25.1}$, $10^{14.3}$, and $10^{10.65}$, respectively. The binding constant of Ca^{2+} indicates that it will not displace either oxidation state of iron from EDTA. In this manner, calcium may act as a pro-oxidant by associating with excess ligand reducing the ligand:metal ratio of EDTA and iron to unity and therefore promoting Fenton reactive conditions. The ligands selected for this study were (EDTA, $(\text{HOOCCH}_2)_2\text{NCH}_2\text{CH}_2\text{N}(\text{CH}_2\text{COOH})_2$, nitrilotriacetic acid (NTA, $\text{N}(\text{CH}_2\text{COOH})_3$), citrate ($\text{HOC}(\text{COOH})(\text{CH}_2\text{COOH})_2$) and glutamate (Glu, $\text{HOOCCH}_2\text{CH}_2\text{CH}(\text{NH}_2)\text{COOH}$). The first two ligands were selected for their well-characterized binding constants, and for their ability to mimic physiological binding sites, e.g. proteins. Citrate is an important LMW ligand for many physiological metal ions and is also involved in the formation of ROS through its various metal complexes (Lobner *et al.* 2003, Harris *et al.* 2003, Chiueh 2001). Glutamate along with Ca^{2+} is part of the excitotoxin response of inflammation. Excessive glutamate has been found to lead to the death of nerve cells. It is interesting to note out of the 20 simple amino acids glutamate has the highest binding constant for Fe^{II} , Fe^{III} , and Ca^{2+} ($10^{3.52}$, $10^{12.1}$, and $10^{1.52}$, respectively). Although not mentioned in the literature, it seems plausible that the purpose of the glutamate release is as a LMW ligand for iron in order to accelerate the oxidative processes.

Experimental

Chemicals: Ferric nitrate nonahydrate (Fisher Chemicals, ACS Grade), citric acid anhydrous (Fisher Chemicals, ACS Grade), calcium nitrate tetrahydrate (Fisher Chemicals, ACS Grade), ethylenediaminetetraacetic acid tetrasodium salt (EDTA) (Acros, 99%), nitrilotriacetic acid (NTA) (Acros, 99%), zinc nitrate hexahydrate (Fisher Chemicals, ACS Grade), d,l-Glutamic acid monohydrate (Glu) (Acros, 99%), hydrogen peroxide (Fisher Chemicals, 31.4%).

Instrumentation: BAS CV-50W potentiostat was used with a 5 mm glassy carbon working electrode, Ag/AgCl reference electrode, and a graphite rod counter electrode.

Stock Solutions: Solutions of Fe^{III} EDTA and Fe^{III} citrate were made up in 0.10 M HEPES(aq) buffer adjusted to pH 7.4. For Fe^{III}NTA and Fe^{III}Glu, all stock and test solutions were made up in 0.010 M HEPES(aq) buffer adjusted to pH 7.4 and 0.10 M NaNO₃(aq). Ca(NO₃)₂ and Zn(NO₃)₂ solutions were made in the same solvent-buffer system as the corresponding Fe^{III}L solutions.

Electrocatalytic H₂O₂ Reduction Experiments: A 1 mL aliquot of 1 mM Fe^{III}EDTA(aq) (1:10) and 1 mL or less of 10 mM Ca(NO₃)₂(aq) were added to 7 mL of aqueous buffer solution and purged with N₂ for 10 to 15 min, after which 1 mL of 230 mM H₂O₂(aq) (purged) was added. The final volume was adjusted to 10 mL with DI water (N₂ purged). Cyclic voltammetry was then conducted at 25, 10 and 5 mV/s from 400 mV to -700 mV. The same procedure was conducted with all Fe^{III}L complexes. The Fe^{III}L ratios for Fe^{III} citrate, Fe^{III}NTA, and Fe^{III}Glu were 1:50, 1:20, and 1:10, respectively.

Generation of pH Distribution Diagrams: All metal complex speciation diagrams were generated by the computer program Hyperquad Speciation and Simulation, HySS (Alderighi *et al.* 1999). Stability constants were obtained from the National Institute of Science and Technology database.

Results

Figure 1 demonstrates the cyclic voltammetric characteristics of Fe^{II/III}EDTA in pH 7.4 0.1 M HEPES buffer remains constant in the presence of varying quantities of ligand. Furthermore, the voltammetric characteristics were unchanged under conditions where the electron transfer kinetics are challenged

($v = 10$ V/s, $\Delta E_p = 245$ mV), indicating that under conditions of high Fe^{II}EDTA turnover the voltammetric characteristics are not a function of EDTA concentration. Identical results were found for NTA, citrate, and glutamate ligands. On the other hand, the ability to drive the Fenton reaction is highly dependent on the [L]:[M] ratio (Bobier *et al.* 2003). This ability of a complexed Fe^{II} species to drive the reaction was examined by cyclic voltammetry (Zhao *et al.* 1994, Bobier *et al.* 2003, Chen & Breen 2000, Bard & Faulkner 2001). Figure 2 demonstrates the sensitivity of the Fenton reaction characteristics to that [L]:[M] ratio. The inset within Figure 2 illustrates the classical sigmoidal shape voltammogram indicative of the EC' case where the reduced substrate, H₂O₂ is freely diffusing (Bard & Faulkner 2001).

Electrochemical, E: Fe^{III}EDTA + e → Fe^{II}EDTA (2)

Catalytic, C': Fe^{II}EDTA + H₂O₂ → Fe^{III}EDTA + HO⁻ + HO[•] (3)

The cathodic wave is nearly steady-state and greatly amplified over Figure 1 because of the combination of Equations 2 and 3 above. That sigmoidal shape is lost in high ratios of [H₂O₂]:[Fe^{III}] and is attributable to the formation of a Fe^{III}-OO²⁻ complex, which takes on the shape curve A in Figure 2 (Bobier *et al.* 2003). The modified EC' voltammogram thus is due to the following mechanism:

Electrochemical, E: Fe^{III} - OO[EDTA] + e → Fe^{II} - OO[EDTA] (2a)

Catalytic, C': Fe^{II} - OO[EDTA] + 2H⁺ → Fe^{III}EDTA + HO⁻ + HO[•] (3a)

Both the inset voltammogram and curve A of Figure 2 exhibit an amplified cathodic wave, which is produced by the electrochemical-catalytic (EC') mechanism. Reaction 2 and 2a produce the Fe^{II} complex, which is consumed in the Fenton reaction (Reaction 3 and 3a). The production of the reactant, Fe^{III}EDTA in the vicinity of the electrode surface enhances the cathodic current via reaction 2/2a. The absence of a cyclic voltammetry anodic wave is a result of the complete consumption of Fe^{II}EDTA in reaction 3. The Fe^{II/III}EDTA couple acts as the redox cycling intermediate for the catalytic reduction of H₂O₂. Cyclic voltammetry in this investigation focused on the high [H₂O₂]:[Fe^{III}EDTA] cases since it is thought that this mimics physiological conditions (0.1 μM

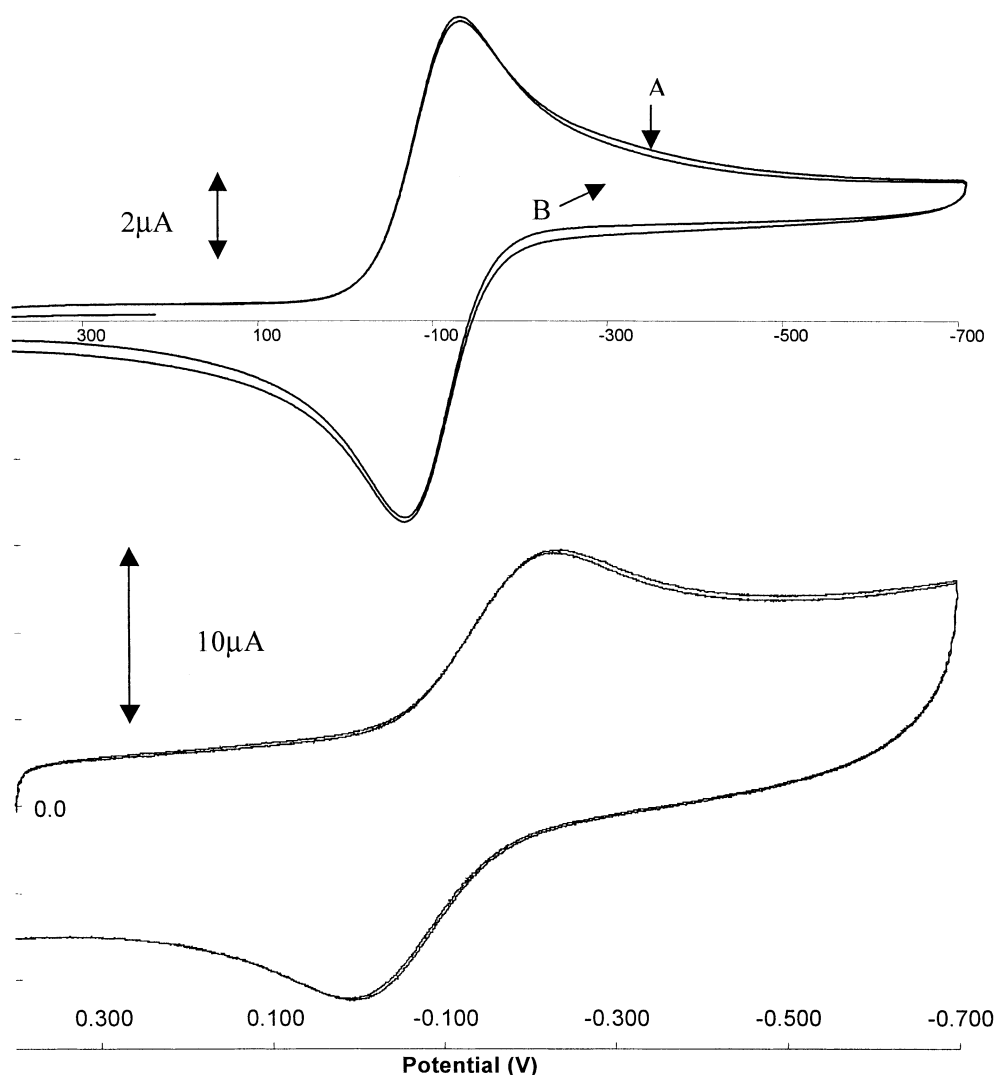


Figure 1. Cyclic voltammograms of $\text{Fe}^{\text{III}}\text{EDTA}$ in 0.1 M HEPES pH 7.4 and 10 mV/s (top) and 10 V/s (bottom) at a carbon disk electrode under conditions of 1.0 mM Fe^{III} , 1.0 mM EDTA and of 1.0 mM Fe^{III} , 10.0 mM EDTA.

ROS; 0.1 nM $\text{Fe}^{\text{II/III}}$). When an excess of Ca^{2+} was added ($[\text{Fe}^{\text{III}}]:[\text{EDTA}]:[\text{Ca}^{2+}]$, [1]:[1]:[10]), the Fenton reaction characteristics of $\text{Fe}^{\text{II}}[\text{EDTA}]$ were unchanged, and the cyclic voltammetric results were the same as Curve A of Figure 2.

Curve B of Figure 2 demonstrates that Fenton reaction of the $\text{Fe}^{\text{II}}\text{EDTA}$ complex is nearly lost in the excess of EDTA ligand. The EC' current drops to nearly the control current observed for the reduction of H_2O_2 in the absence of a $\text{Fe}^{\text{II/III}}\text{EDTA}$ mediator couple in curve D of Figure 2. This was consistent with a previous study and is the hypothesis as to how EDTA and related ligands have both pro-oxidant and antioxidant features (Bobier *et al.* 2003).

The addition of Ca^{2+} (as $\text{Ca}(\text{NO}_3)_2$) to the solution of 1:10 $[\text{Fe}^{\text{III}}]:[\text{EDTA}]$ increases the Fenton reaction characteristics of the iron-EDTA complex. This is demonstrated by curve C of Figure 2 where Ca^{2+} is added to a ratio of 1:1 $[\text{Ca}^{2+}]:[\text{EDTA}]$. The EC' catalytic wave returns to $\approx 60\%$ of its maximum of the 1:1 $[\text{Fe}^{\text{II/III}}]:[\text{EDTA}]$ complex in curve A of Figure 2 at the switching potential of -700 mV. It is noteworthy that none of the observed effects were attributable to an artifact in the differences in electron transfer kinetics of the 1:1 and 1:10 $[\text{Fe}^{3+/2+}]:[\text{EDTA}]$. This is evident in the study described by Figure 1. The recovery of iron complex Fenton Reaction activity by the addition

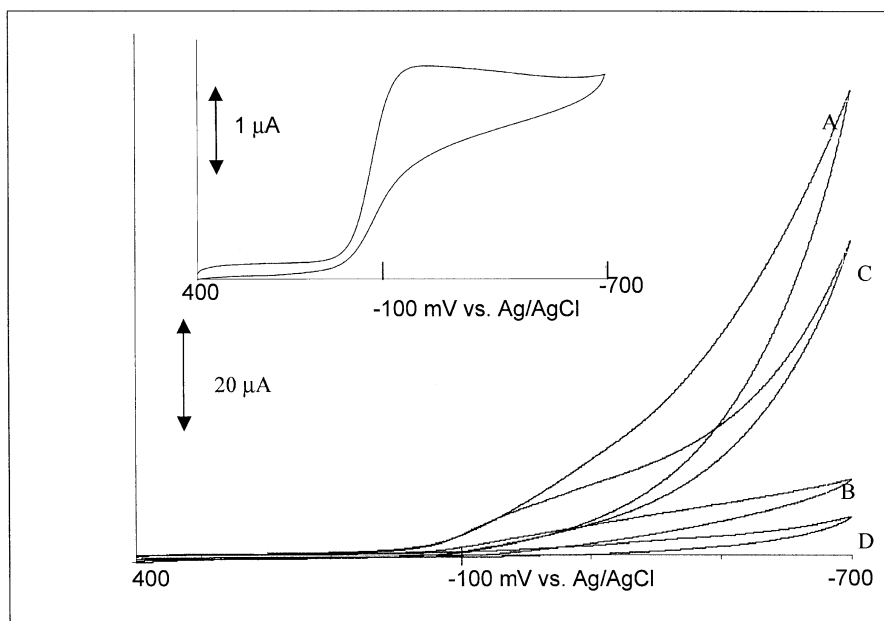


Figure 2. Electrocatalytic reduction of 22.8 mM H_2O_2 0.1 mM Fe^{III} under conditions of various ratios of $[\text{Fe}^{\text{III}}]:[\text{EDTA}]:[\text{Ca}^{2+}]$.

Curve A: [1]:[1]:[0] & [1]:[1]:[10]

Curve C [1]:[10]:[10]

Curve B [1]:[10]:[0]

Curve D blank [0]:[0]:[0] & [0]:[0]:[1]

Inset: Electrocatalytic reduction of 1 mM $\text{H}_2\text{O}_2(\text{aq})$ in the presence of 0.1 mM Fe^{III} EDTA (1:1). Other conditions pH 7.4 HEPES, carbon disk electrode, 10 mV/s sweep rate.

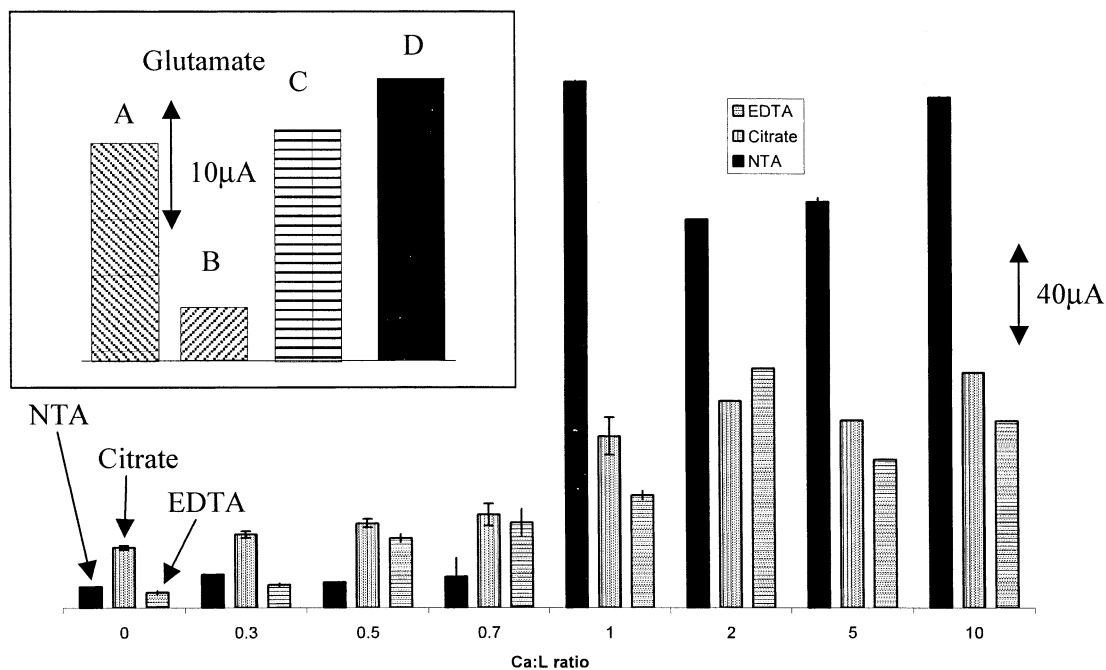


Figure 3. Inset – Electrocatalytic reduction of H_2O_2 under conditions of various ratios of $[\text{Fe}^{3+}]:[\text{Glu}]:[\text{Ca}^{2+}]$.

Curve A: [1]:[5]:[0]

Curve C [1]:[15]:[0]

Curve B [1]:[10]:[0]

Curve D [1]:[10]:[10]

Bottom – Recovery of Fenton reactivity of Fe complexes by addition of Ca^{2+} .

1:50 $[\text{Fe}^{3+}]:[\text{citrate}]$

1:20 $[\text{Fe}^{3+}]:[\text{NTA}]$

1:10 $[\text{Fe}^{3+}]:[\text{EDTA}]$.

Other conditions 0.1 mM Fe^{3+} , 22.8 mM H_2O_2 and pH 7.4 HEPES, carbon disk electrode, 10 mV/s sweep rate.

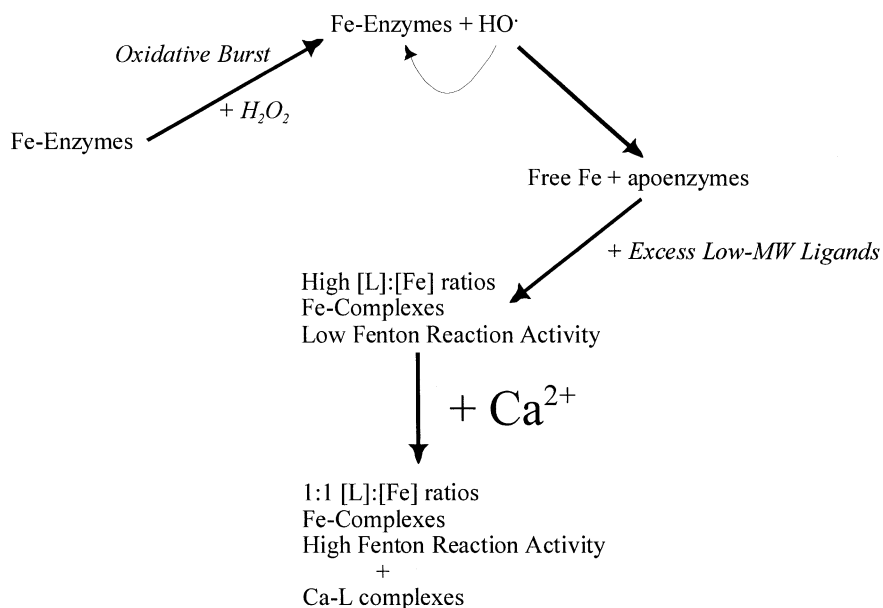


Figure 4. A schematic of the role of calcium in the oxidative burst mechanism.

of excess Ca^{2+} was also observed with citrate, NTA and Glutamate chelates.

Figure 3 demonstrates the recovery of Fenton reactivity of high [ligand]:[metal] ratios by addition of Ca^{2+} . The inset of Figure 3 demonstrates the loss of Fenton Reaction activity as measured by the method of Figure 2 for the Fe^{III} Glu complex. The optimal EC' current measured at -700 mV corresponds to the 1:5 $[\text{Fe}^{\text{III}}]:[\text{Glu}]$ ratio (Bar A, Figure 3). This is reduced by 80% when the $[\text{Fe}^{\text{III}}]:[\text{Glu}]$ ratio is increased to 1:10 (Bar B, Figure 2). The measured EC' current at -700 mV Ag/AgCl for the 1:10 $[\text{Fe}^{\text{III}}]:[\text{Glu}]$ increased with addition of Ca^{2+} (Bars C and D of Figure 2). Bar C of Figure 3 indicates that the 1:10 $[\text{Fe}^{\text{III}}]:[\text{Glu}]$ complex reaches the efficiency of the 1:5 $[\text{Fe}^{\text{III}}]:[\text{Glu}]$ (Bar A) when there is a presence of 10:10 $[\text{Ca}^{2+}]:[\text{Glu}]$ ratio. The major body of Figure 3 indicates that all four complexes experience increasing quantities of Fenton reaction activity by increasing the Ca^{2+} concentration. The 1:50 $[\text{Fe}^{\text{III}}]:[\text{citrate}]$, 1:20 $[\text{Fe}^{\text{III}}]:[\text{NTA}]$, & 1:10 $[\text{Fe}^{\text{III}}]:[\text{EDTA}]$ ratios represent the minimums for the Fenton Reaction activity through the measured EC' currents at -700 mV Ag/AgCl. It was generally observed that full Fenton Reactivity was recovered when added Ca^{2+} reached 1:1 $[\text{Ca}^{2+}]:[\text{ligand}]$ ratio. Increasing that ratio does not affect this observation, (see Figure 3).

Discussion

The preference for carboxylate/oxygen ligands over N and S containing species by Ca^{2+} is based on its hard ion nature (Forsén & Kördel 1994). Iron(III) ions share such behavior, hence the propensity to compete for similar physiological chelation spheres. Such spheres are expected to be present in the plethora of peptides, proteins, and nucleotides present in cellular systems containing hard O^- sites; hence the choice of EDTA, NTA, citrate and glutamate as analogues to these physiological chelation sites.

A schematic of the possible role of Ca^{2+} release in the inflammatory response is shown in Figure 4. As discussed in the Introduction, under conditions of oxidative stress the concentration of labile iron greatly increases (Petrat *et al.* 2002, Kakhlon & Cabantchik 2002, Galley & Webster 1996, Gutteridge *et al.* 1996a, b). This is from the release of Fe ions from its native enzymatic shell through destruction by oxidative processes (Walling *et al.* 1970, Avila *et al.* 2000, Collins 2002, Comporti *et al.* 2002, Richards & Dettman 2003, Lipscomb *et al.* 1998). Despite this release it can be expected that the conditions for oxidative damage will be compromised. The LMW chelation pool of physiological fluids can be reasonably expected to be in much greater concentration than labile iron ($\approx \text{nM}$), hence the strong possibility for the less than optimal Fenton reaction performance (Bobier *et al.* 2003). This

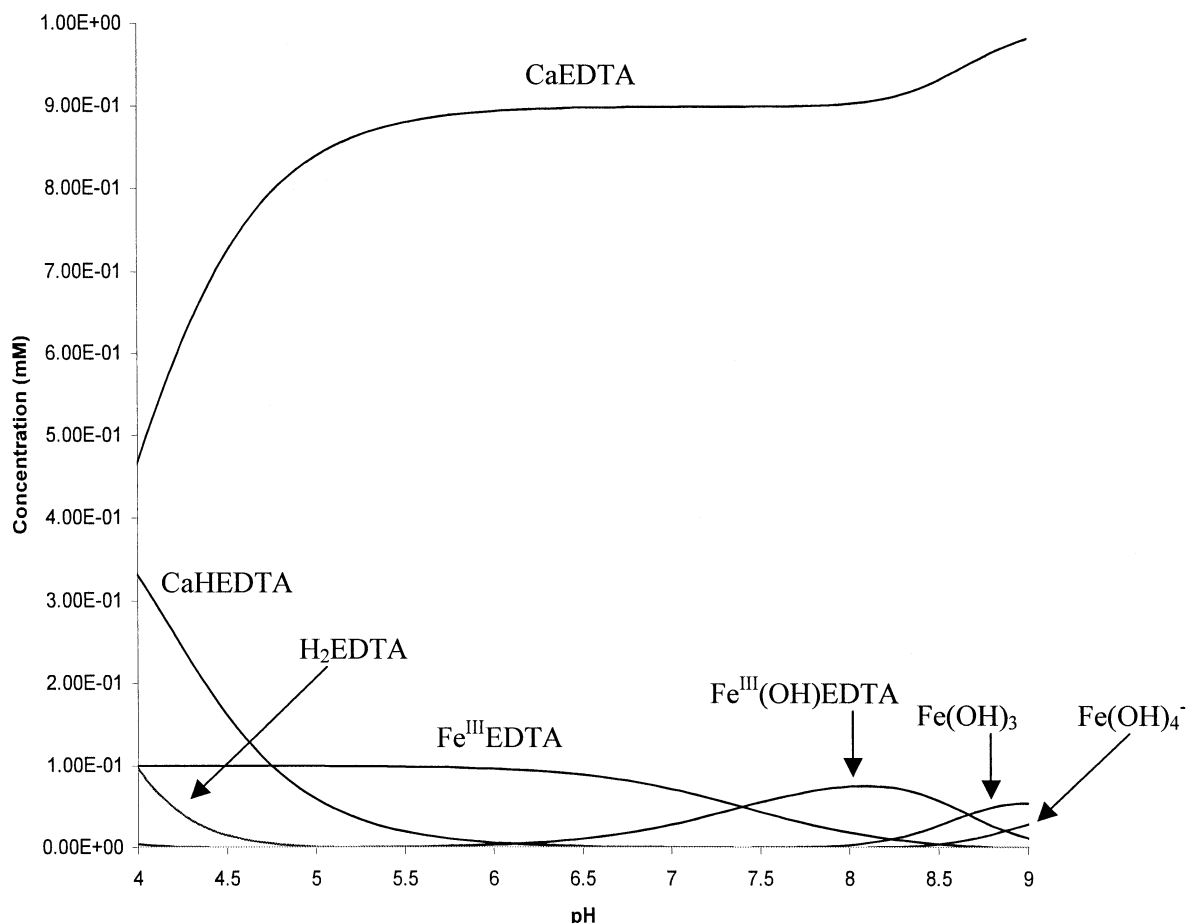


Figure 5. pH distribution diagram of Ca and Fe^{III}EDTA complexes, 1:10:100 [Fe^{III}][EDTA][Ca²⁺], 0.1 mM Fe³⁺, 1 mM EDTA, 10 mM Ca²⁺. Free Ca²⁺ is omitted (≈ 9 mM).

is evident in the studies summarized in Figures 2 and 3 with EDTA, NTA, citrate, and glutamate and in a previous study with DTPA (Bobier *et al.* 2003). The introduction of Ca²⁺, greatly improves the Fenton reaction characteristics of the Fe complex under high [L]:[M] ratios. The release of Ca²⁺ in the intracellular fluid can be expected to behave in the same way, i.e. the uptake of excess hard O⁻ ligand sites, thus lowering the activation barrier by allowing for the formation of the FeIII-OO[EDTA] complex.

The release of Ca²⁺ does not displace either Fe^{II} or Fe^{III} from their respective chelation spheres. Both Fe^{II}EDTA ($\log \beta_1 = 14.3$) and Fe^{III}EDTA ($\log \beta_1 = 25.1$) have significantly higher stability constants than CaEDTA ($\log \beta_1 = 11$). The pH distribution diagrams calculated from the respective iron EDTA stability and hydrolysis constants and are presented in Figure 5. Figure 5 demonstrates that under the con-

ditions of equimolar concentrations of Fe^{III}, EDTA, and Ca²⁺, the mono-hydroxy Fe^{III}-EDTA complex predominates at pH 6.5 to 8.5. Under conditions of 100:10:1 [Ca²⁺]:[EDTA]:[Fe³⁺], the mono-hydroxy Fe^{III}-EDTA complex again remains intact, whereas the excess EDTA is taken up by Ca²⁺. This situation remains mostly intact up to a 10000:10:1 ratio of [Ca²⁺]:[EDTA]:[Fe³⁺]. Figure 6 demonstrates again that Fe²⁺ chelation by EDTA is not displaced by excess Ca²⁺. This indicates that Ca²⁺ takes up excess ligand leaving an optimal [L]:[M] ratio for maximum Fenton reaction activity.

The possibilities for other metal ions acting in a similar manner must be considered. Another common hard physiological ion, Mg²⁺, prefers the formation of octahedral complexes. On the other hand, Ca²⁺ has the ability to form complexes of 6, 7, 8, and 9 ligands. This flexibility enables Ca²⁺ to bind to multident-

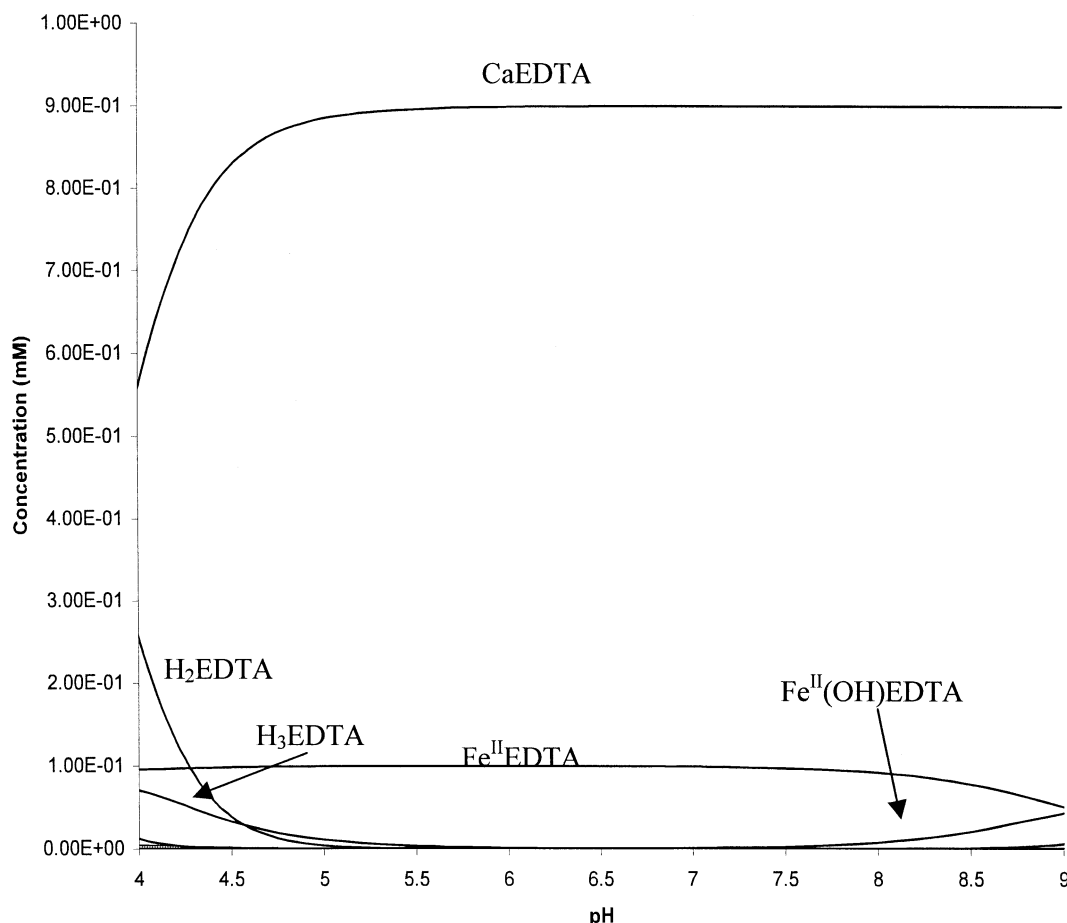


Figure 6. pH distribution diagram of Ca and Fe^{II}-EDTA complexes, 1:10:100 [Fe^{II}][EDTA] [Ca²⁺], 0.1 mM Fe²⁺, 1 mM EDTA, 10 mM Ca²⁺. Free Ca²⁺ is omitted (≈ 9 mM).

ate ligands more efficiently than Mg²⁺. For example, the stability constants for Mg²⁺ and Ca²⁺ binding to EDTA are $10^{8.8}$ and $10^{10.6}$, respectively. The binding constant of Ca²⁺ to the Glu-Glu peptide is $10^{3.2}$ with no binding to Mg²⁺ (Forsén & Kördel 1994). Furthermore, the rates in which the hydration sphere is displaced by ligands is faster for Ca²⁺ in comparison with Mg²⁺, $\log k(s^{-1})$ 8.4 vs. 5.2, respectively (Frey & Stueher 1974). These characteristics indicate that Ca²⁺ would be preferred over Mg²⁺ in the optimization for the pro-oxidant effects of LMW-Fe species.

In summary, a new hypothesis is presented regarding an as of yet unexplored possibility for the pro-oxidant action Ca²⁺. This is based on the optimization of Fe chelation sphere by taking up excess iron ligand, which improves the kinetics for the Fenton reaction by allow for the formation of Fe^{III}-OO[EDTA]. In future

investigations we will examine the ability of excess chelate to prevent the formation of Fe-OO[EDTA].

Acknowledgements

Mark D. Engelmann and Ryan Hutcheson acknowledge summer support from Malcom Renfrew Scholarship Fund. Funding is provided by the National Institutes of Health grant number R15 GM062777-01

References

- Alderighi L, Gans P, Ienco A, Peters D, Sabatini A, Vacca A. 1999 'Hyperquad simulation and speciation (HySS): a utility program for the investigation of equilibria involving soluble and partially soluble species', *Coord Chem Rev* **184**: 311–318
- Arouma OI, Halliwell B. 1988 'The Iron-Binding and Hydroxyl Radical Scavenging Action of Anti-inflammatory Drugs', *Xenobiotica*, **18**: 459–470

- Atlante A, Calissano C, Bobba A, Giannatassio S, Marra E, Passarella S. 2001 'Glutamate Neurotoxicity, Oxidative Stress, and Mitochondria.' *FEBS Letters* **497**: 1–5
- Avila L, Huang H, Rodriguez JC, Moënn-Loccoz, P, Rivera M. 2000 'Oxygen Activation by Axial Ligand Mutants of Mitochondrial Cytochrome b₅: Oxidation of Heme to Veroheme and Bilverdin' *J Am Chem Soc* **122**: 7818–7619
- Babior BM. 2000 'Phagocytes and Oxidative Stress' *Amer J Med* **109**: 33–44
- Bard AJ, Faulkner LR. 2001 In: *Electrochemical Methods: Fundamentals and Applications*, 2nd Edition. John Wiley and Sons, New York, p. 501?
- Berlett BS, Chock PB, Yim MB, Stadtman ER. 1990 'Manganese(II)-bicarbonate-mediated catalytic activity for hydrogen peroxide dismutation and amino acid oxidation: detection of free radical intermediates.' *Proc Nat Acad Sci USA* **87**(1): 389–393.
- Blokhina O, Virolainen E, Fagerstedt KV. 2003 Antioxidants, Oxidative Damage and Oxidation Deprivation Stress: a Review' *Ann Bot* **91**: 179–194
- Bobier RT, Engelmann MD, Hiatt T, Cheng IF. 2003 'Variability of the Fenton Reaction Characteristics of the EDTA, DTPA, and Citrate Complexes of Iron' *Biometals* **16**: 519–527
- Caro AA, Cederbaum AI. 2002a 'Role of Calcium-activated Proteases in CYP2E1- dependent Toxicity in HEPG2 Cells' *J Biol Chem* **277**: 104–113
- Caro AA, Cederbaum. 2002b A.I. 'Ca²⁺-dependent and Independent Mitochondrial Damage in HepG2 Cells that Overexpress CYP2E1' *Arch Biochem Biophys* **408**: 162–170
- Cheng IF, Breen K. 2000 'On the Ability of Four Flavanoids, Baiciclein, Luteolin, Naringenin and Quercetin, to Suppress the Fenton Reaction of the Iron-ATP Complex.' *Biometals* **13**: 77–83
- Chiueh CC. 2001 'Iron overload, oxidative stress, and axonal distrophy in brain disorders.' *Pediatr Neurol* **25**(2): 138–47
- Collins TJ. 2002 'TAML oxidant activators: a new approach to the activation of hydrogen peroxide for environmentally significant problems.' *Acc Chem Res* **35**: 782–90
- Comporti M, Signorini C, Buonocore G, Ciccoli L. 2002 'Iron release, oxidative stress and erythrocyte ageing.' *Free Radic Biol Med* **32**: 568–76
- Crichton RR, Pierre J-L. 2001 'Old Iron, Young Copper: fro Mars to Venus' *Biometals* **14**: 99–112
- Fahn S, Cohen G. 1992 'The oxidant stress hypothesis in Parkinson's disease: evidence supporting it.' *Ann of Neurol* **32**: 802–812
- Forsén S., Kördel J. 1994 Calcium in Biological Systems, In: Bertini I, Gray HB, Lippard SJ, Valentine JS, eds *Bioinorganic Chemistry*, University Science Books, Mills Valley, California, Chapter 3.
- Frey CM, Stuehr J. 1974, in *Metal Ions in Biological Systems*, Sigel H, ed. Marcel Dekker, New York, 1, 51.
- Galley HF, Webster NR. 1996 'Elevated serum bleomycin-detectable iron concentrations in patients with sepsis syndrome.' *Intensive Care Med* **22**: 226–229
- Gutteridge JMC, Mumby S, Koizumi M, Taniguchi N. 1996a 'Free Iron in Neonatal Plasma Activates Aconitase: Evidence for Biologically Reactive Iron' *Biochem Biophys Res Comm* **229**: 806–809
- Gutteridge JMC, Mumby GJ, Quinlan GJ, Chung KF, Evans TW. 1996b 'Pro-oxidant Iron in Human Pulmonary Epithelial Lining Fluid: Implications for Oxidative Stress in the Lung.' *Biochem Biophys Res Comm* **220**: 1024–1027
- Harris WR, Wan Z, Brook C, Yang B, Islam A. 2003 'Kinetics of Metal Ion Exchange between Citric Acid and Serum Transferrin.' *Inorg Chem* **42**(19): 5880–5889
- Kakhlon O, Cabantchik ZI. 2002 'The labile iron pool: characterization, measurement, and participation in cellular processes' *Free Radic Biol Med* **33**: 1037–46
- Krebs J. 1998 'The Role of Calcium in Apoptosis' *Biometals* **11**: 375–382
- Lee C-C, Kang J-J. 2002 'Extract of Motorcycle Exhaust Particles Induced Macrophages Apoptosis by Calcium-Dependent Manner' *Chem Res Toxicol* **15**: 1534–1542
- Lehnen-Beyel I, Groot HD, Rauen U. 2002 'Enhancement of iron toxicity in L929 cells by D-glucose: accelerated(re-)duction.' *Biochem J* **368**(Pt2): 517–26
- Lipscomb DC, Gorman LG, Traystman RJ, Hurn PD. 1998 'Low molecular weight iron in cerebral ischemic acidosis in vivo.' *Stroke* **29**: 487–492
- Lobner D, Golner S, Hjelmhaug J. 2003 'Neurotrophic factor effects on oxidative stress-induced neuronal death.' *Neurochem Res* **28**(5): 749–56
- Petrat F, de Groot H, Sustmann R, Rauen U. 2002 'The chelatable iron pool in living cells: a methodically defined quantity.' *Biol Chem* **383**(3–4): 489–502
- Richards MP, Dettman MA. 2003 'Comparative Analysis of Different Hemoglobins: Autoxidation, Reaction with Peroxide, and Lipid Oxidation.' *J Agric Food Chem* **51**: 3886–3891
- Sergeant O, Anger JP, Lescoat G, Pasdeloup N, Gillard P, Cillard J. 1997 'EPR determination of low molecular weight iron content applied to whole rat hepatocytes.' *Cell Molec Biol* (Noisy-le-grand) **43**: 793–800
- Shi X, Dalal NS, Jain AC. 1991 'Antioxidant Behavior of Caffeine: Efficient Scavenging of Hydroxyl Radicals.' *Food Chem Toxicol* **29**: 1–6
- Smith MA, Harris PL, Sayre LM, Perry G. 1997 'Iron Accumulation in Alzheimer Disease is a Source of Redox Generated Free Radicals.' *Proc Nat Acad Sci USA* **94**: 9866–9868
- Walling C, Kurz M, Schugar HJ. 1970 'The Iron(III)-Ethylenediaminetetraacetic Acid-Peroxide System' *Inorg Chem* **9**(4): 931–937
- Wang J, Ortiz De Montellano PR. 2002 'The binding sites on human heme oxygenase-1 for cytochrome P450 reductase and biliverdin reductase.' *J Biol Chem* in press 2003
- Welch KD, Davis TZ, Van Eden ME, Aust SD. 'Deleterious iron-mediated oxidation of biomolecules.' *Free Radic Biol Med* **32**: 577–83
- Wiseman H, Halliwell B. 1996 'Damage to DNA by Reactive Oxygen and Nitrogen Species: Roles in Inflammatory Disease and Progression to Cancer.' *Biochem J* **313**: 17–29
- Weaver J, Pollack S. 1989 'Low-Mr iron isolated from guinea pig reticulocytes as AMP-Fe and ATP-Fe complexes.' *Biochem J* **261**: 787–792
- Weaver J, Pollack S. 1990 'Two types of receptors for iron on mitochondria.' *Biochem J* **271**: 463–466
- Zhan H, Gupta RK, Weaver J, Pollack S. 1990 'Iron bound to low MW ligands: interactions with mitochondria and cytosolic proteins.' *Europ J Haematol* **44**: 125–131
- Zhao CP, Galazka M, Cheng IF. 1994 'Electrocatalytic Reduction of Hydrogen Peroxide by Iron-Adenosine Nucleotide Complexes.' *J Electroanal Chem* **379**: 501–503